Removal of chloridazon pesticide from waters by Fenton and photo-Fenton processes

Hatice Bike Ulu[a], Nejdet Değermenci[a], Filiz B. Dilek[b],*

[a]*Department of Environmental Engineering, Kastamonu University, Kastamonu, Turkey, emails: hbicen@kastamonu.edu.tr (H. Bike Ulu), degermenci@kastamonu.edu.tr (N. Değermenci)*
[b]*Department of Environmental Engineering, Middle East Technical University, Ankara, Turkey, email: fdilek@metu.edu.tr (F.B. Dilek)*

ABSTRACT

Chloridazon (CLZ), also named as Pyrazon and classified as organochlorine pesticides, is widely used during sugar beets cultivation. CLZ being a pesticide with high solubility in water is likely to end up in surface and groundwater bodies because of its high mobility in soil. Due to its toxic properties, it may cause serious problems in human health and ecological cycle. In the present study, the removal of CLZ pesticide by Fenton and photo-Fenton processes was investigated. The effects of parameters such as H_2O_2, Fe(II), initial CLZ concentration, pH, and temperature were studied. It was observed that CLZ completely disappeared within 1 h and 20 min by the Fenton and photo-Fenton process, respectively, under optimal conditions. The optimal conditions for each processes were attained as 7.5 mg/L Fe(II), 50 mg/L H_2O_2, 40 mg/L initial CLZ, pH 3 and 20°C for Fenton process, and 5 mg/L Fe^{2+}, 50 mg/L H_2O_2, 60 mg/L initial CLZ, pH 3 and 20°C for photo-Fenton process. The reaction kinetics of CLZ followed Behnajady–Modirdhahla–Ghanbery kinetic model. Desphenyl CLZ, pyridazine-3,4,5-trione, oxaluric acid, and 5-hydroxyhydantion were identified as CLZ degradation by-products. Accordingly, the degradation pathway was proposed.

Keywords: Chloridazon removal; Fenton; Photo-Fenton; Kinetics; By-products

1. Introduction

Pesticides, rank first in the category of micropollutants due to excessive and widespread uses, are the chemicals used to destroy weeds and insects that damage plants and to prevent plant diseases. Although the goal is to increase the yield of agricultural products, it is now evident that there are so many harmful effects on the environment and human health. Based on their categories and half-life for each pesticide, they persist, accumulate, and transport in soil and water for many years. These toxic, low-biodegradable, and water-soluble chemicals can cause serious environmental pollution due to infiltration to surface and groundwater. Notably, water resources close to agricultural areas contain pesticide residues, and the consumption of these resources may have severe risks to humans [1].

Chloridazon (5-amino-4-chloro-2-phenyl-3(2H)-pyridazinone) is a pesticide belonging to the pyrazinone family. It is used before and after planting the sugar beets to combat the broad-leaved weeds of beet cultivars as a barrier to photosynthesis. Chloridazon (CLZ) can easily be transported in various media owing to its high organic carbon-water partitioning coefficient (K_{oc}) and low octanol-water partitioning coefficient (K_{ow}). Therefore, it has a high potential to enter the surface and groundwater [2]. Nevertheless, CLZ removal from waters took a tiny place in the literature. In a few studies, adsorption [3], photolysis with titanium dioxide [4], and ozonation [5] have been applied for the removal

---

* Corresponding author.

of this pesticide but the removal efficiencies attained were quite variable, ranging from 5% to 100%. Besides being in limited numbers, they are not sufficiently detailed studies, except the one by Azaari et al. [6] who investigated the possible by-products of CLZ degradation during photolysis with titanium dioxide. So, there is a need to study further toward the removal of CLZ from waters.

Recently, several studies put forward that advanced oxidation processes (AOPs) are the most efficient method for the treatment of wastewaters containing pesticides [7–12]. AOPs rely on the formation of hydroxyl radicals ($OH^{\bullet}$) with high oxidant properties and provide efficient treatment. These radicals are an exceptional type of oxidant and known as the best one (2.8 V) after the fluorine oxidant [13]. The advantage of AOPs overall chemical and biological processes is that they do not transfer pollutants from one phase to the other (as in chemical precipitation and adsorption) or do not produce high amounts of sludge [14].

Fenton Oxidation, as one means of AOPs, relies on the $OH^{\bullet}$ formed by the mixture of hydrogen peroxide (H_2O_2) and iron salts (Fe^{2+}) as shown in Eq. (1) [15,16].

$$Fe^{2+} + H_2O_2 \rightarrow Fe^{3+} + OH^- + OH^{\bullet} \qquad (1)$$
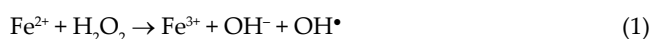
In photo-Fenton oxidation, UV irradiation contributes to the formation of $OH^{\bullet}$ by photolysis of Fe(III) complex ions and H_2O_2 as shown in Eq. (2). In the presence of H_2O_2, the regenerated Fe(II) from the photolysis of Fe(III) species is oxidized by H_2O_2 and produces a new $OH^{\bullet}$. Thus, the oxidation of organic compounds will accelerate [17].

$$Fe^{3+} + H_2O_2 + h\nu \rightarrow Fe^{2+} + H^+ + OH^{\bullet} \qquad (2)$$
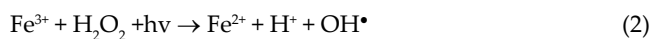
In the present study, the degradation of CLZ in water by Fenton and photo-Fenton processes were investigated. To this purpose, the effects of operational parameters, such as pH, temperature, H_2O_2, Fe(II), and initial CLZ concentrations were sought. In this respect, a series of batch experiments were performed within the specified ranges of these parameters to allow a systematic parametric study. CLZ removal kinetics were also examined for each treatment application, and kinetic model analysis was performed. Additionally, by-products formation was sought.

2. Materials and methods

2.1. Pesticide studied

A pesticide CLZ is used in this study. This pesticide is obtained commercially from the product Pyrazon, which contains 65% of CLZ as an active compound. The physicochemical properties of CLZ are as presented in Table 1 [18].

2.2. Other chemicals used

The analytical grade of CLZ (≥97% purity) (used as a standard solution in high-performance liquid chromatography (HPLC) method), sodium hydroxide (NaOH), sulphuric acid (H_2SO_4), iron sulfate heptahydrate ($FeSO_4 \cdot 7H_2O$) and hydrogen peroxide (H_2O_2) were supplied from Sigma-Aldrich, (Germany). Other chemicals, including sodium

Table 1
Physical properties of CLZ

Name of Properties	Details
Chemical name	Chloridazon (5-amino-4-chloro-2-phenyl-3(2H)-pyridazinone)
Synonym	Pyrazon
Molecular formula	$C_{10}H_8ClN_3O$
CAS number	1698-60-8
Appearance	Crystalline, Colorless
Molecular weight (g/mol)	221.6
Water solubility (mg/L)	422
Density (kg/L)	1.54
$\log K_{ow}$	1.2
K_{oc}	89–340
Dissociation constant pKa	3.38
Vapor pressure	4.50×10^{-7} mmHg at 20°C
Half-life (d)	105

sulfite (Na_2SO_3) (>98%), potassium iodide (KIO_3), potassium triiodide (KI_3) were purchased from Tekkim (Turkey). The HPLC grade acetonitrile (>99.9% purity) was obtained from Merck (Germany). All aqueous solutions were prepared with ultrapure distilled water.

2.3. Synthetic water

Experiments were performed using synthetic water prepared by injecting the desired amounts of CLZ from its stock solution (100 mg/L) into the ultra-pure water. The CLZ concentration range studied (20–60 mg/L) is beyond the levels likely to be found in real domestic wastewaters (possibly at μg/L level). But, this level of CLZ could be possible to observe in the discharges of industries producing this pesticide. So, this concentration range could represent such wastewaters. Also, potential degradation by-products would be easily detectable as the by-product concentrations will be higher when the higher influent pesticide is used.

2.4. Experiments

All experiments were performed in a cylindrical jacket glass reactor of 1 L volume (6 cm in width, 26 cm in length). The reactor was placed on the magnetic stirrer, which provides homogenous mixing at 600 rpm. The desired temperature was maintained with the help of a cooling circulator connected to the reactor. During photo-Fenton experimentations, as different from the Fenton oxidation, a UV lamp which is held in a 3 cm quartz bulb is placed in the center of the reactor (Fig. 1). UV lamp used was of 10 W low-pressure mercury (LightTech, Hungary) emitting at 253.7 nm. Before the lamp was placed in the quartz bulb, it was allowed to stand for 15 min to get up to full intensity. In addition, the reactor was covered with aluminum foil so that there will be no loss from the light source. The UV light intensity was measured by the KI/KIO_3 Actinometer method [19] as 1.9912 μEinstein/s.

Before starting the experiments, the reactor was filled with a 600 mL CLZ aqueous solution at the desired
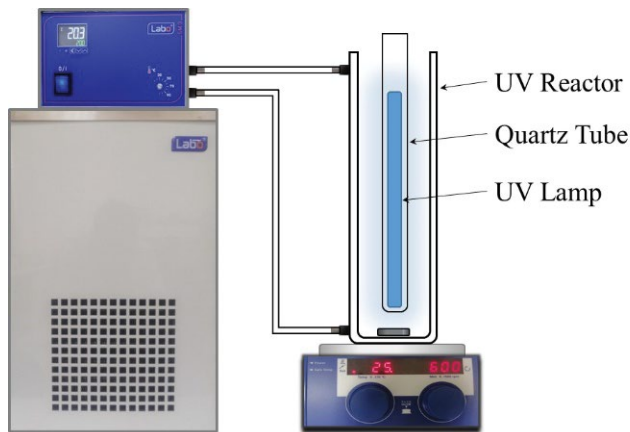
Fig. 1. Experimental setup.

concentration. The pH of the solutions was adjusted with 1 M NaOH or H_2SO_4 solutions. After the pH adjustment, the desired amounts of $FeSO_4 \cdot 7H_2O$ and H_2O_2 were added to the reactor. While determining the concentrations of Fe^{2+} and H_2O_2 to include in the experimental matrix, firstly, ranges provided in the literature data belonging to Fenton's experimentation were considered. It was seen that the ratio of H_2O_2/Fe^{2+} was very variable, depending on the type of pollutants. Therefore, preliminary tests were performed with CLZ and the concentrations of H_2O_2 and Fe^{2+} to be tested were determined. The experimental matrix implemented is given in Table 2 for both Fenton and photo-Fenton processes. Measurements were conducted in duplicate, and arithmetic averages were taken. Moreover, to quench the reactions in Fenton and photo-Fenton processes, 0.1 g Na_2SO_3 was added to each sample taken [20,21].

2.5. Kinetic analysis

During AOPs, degradation kinetics of contaminants is known to follow bimolecular kinetics and hence can be principally described by second-order reaction kinetics [22] [Eq. (3)].

$$\frac{d\left[\text{CLZ} \right]}{dt} = k_2 \left[\text{CLZ} \right] \left[\text{H}_2\text{O}_2 \right] \tag{3}$$

where k_2 is the second-order rate constant, [CLZ] Contaminant concentration, and [H_2O_2] concentration of H_2O_2.

If H_2O_2 is used excessively in the reaction, it will only depend on the CLZ concentration. So, the reaction will follow pseudo-first-order kinetics [23–26] [Eq. (4)].

$$\frac{d\left[\text{CLZ} \right]}{dt} = k_1 \left[\text{CLZ} \right] \tag{4}$$

Another kinetic model, called Behnajady–Modirdhahla–Ghanbery (BMG) kinetic model [Eq. (5)], was also proposed by Behnajady et al. [27] to describe the oxidation of organics by the Fenton process. They stated that the BMG model is simpler and more accurate to forecast the Fenton

process. Conversely, Park et al. [28] claimed that the pseudo-first-order kinetic model can adequately interpret the rapid degradation but not the retarded degradation whereas the BMG model well describes both rapid initial degradation and retarded degradation phases.

$$\frac{C_t}{C_0} = 1 - \left[\frac{t}{\left(m + b_t \right)} \right] \tag{5}$$

where m and b are constants for the oxidation capacities and reaction kinetics, respectively. According to the equation, the slope and the intercept m and b constants can be obtained from the time-dependent $t/[1–(C_t – C_0)]$ graph [28]. These constants can also be determined from the derivation of the main equation of the BMG kinetic model [Eq. (6)].

$$\frac{dC / C_0}{dt} = \frac{-m}{\left(m + b_t \right)^2} \tag{6}$$

In this study, both models mentioned above were tested for Fenton and photo-Fenton oxidation of CLZ.

2.6. Analytical methods

The CLZ concentration was analyzed by HPLC (Shimadzu, LC-20A Prominence, Japan) with HPLC C18 column (4.6 mm × 250 mm), CBM 20A system controller, LC-20A solvent delivery unit, SIL 20A auto-sampler and 225 nm UV-VIS detector (190–800 nm). Ultra-pure water and acetonitrile mobile phases were used at 65% and 35% rates, respectively, at a constant flow rate of 1 mL/min for CLZ analysis in HPLC.

For the analysis of degradation by-products of CLZ, liquid chromatography–mass spectrometry system (LC/MS/MS) device was used. The final LC/MS/MS conditions were; flow rate 0.3 mL/min, temperature 40°C, pressure 100 bar, injection volume 0.3 μL, and 1 min analysis period in positive mode for each analysis. Methanol (5 mM), ammonium format (5 mM), and water were used as mobile phases.

3. Results and discussion

3.1. CLZ removal by Fenton and photo-Fenton processes

Parametric studies were performed for both Fenton and photo-Fenton process. In this respect, the effects of pH, temperature, H_2O_2, Fe^{2+}, and initial CLZ concentration were investigated under the operational conditions presented in Table 2. In the following sections, results obtained are provided and discussed.

3.1.1. Effect of pH

The pH is an important parameter since it plays a vital role in the formation of $OH^{\bullet}$ [29]. In an attempt to investigate the effect of pH on the CLZ removal performance for the Fenton and photo-Fenton processes, a series of experiments were performed under different initial pH conditions, namely, pH 2, 3, 4, and 5. The reason for selecting an acidic pH range lies behind the fact that more $OH^{\bullet}$ will be formed at lower pH [30–32]. Also, the formation of $Fe(OH)_3$

Table 2
Experimental matrix

Fenton process					Photo-Fenton process				
pH	H_2O_2 mg/L	CLZ_0 mg/L	Fe^{2+} mg/L	T °C	pH	H_2O_2 mg/L	CLZ_0 mg/L	Fe^{2+} mg/L	T °C
2	100	40	5	20	2	50	40	5	20
3	100	40	5	20	3	50	40	5	20
4	100	40	5	20	4	50	40	5	20
5	100	40	5	20	3	50	40	2.5	20
3	100	40	2.5	20	3	50	40	7.5	20
3	100	40	7.5	20	3	10	40	5	20
3	100	40	10	20	3	20	40	5	20
3	10	40	5	20	3	50	20	5	20
3	20	40	5	20	3	50	60	5	20
3	50	40	5	20	3	50	60	5	30
3	200	40	5	20	3	50	60	5	40
3	50	10	5	20					
3	50	20	5	20					
3	50	60	5	20					
3	50	40	5	10					
3	50	40	5	30					
3	50	40	5	40					

with a low catalytic property is to occur at higher pH values [33]. Figs. 2a and b show the variation of CLZ concentration with time at each pH condition for the Fenton and photo-Fenton process, respectively.

As shown in Fig. 2a, the highest CLZ removal is attained at pH 3 for both processes, as also supported by the literature studies [34,35]. It can be depicted in Figs. 2a and b that when the pH value was increased from 2 to 3, the removal rate increases, but when the pH was increased to 4, it decreases. This decrease in CLZ removal can be attributed to the possibility of precipitation of iron source as ferric hydroxide, as also stated by Ghaly et al. [36] and Sun et al. [24]. In addition to this, the oxidation ability of $OH^{\bullet}$ could decrease with increasing pH [37]. On the other hand, the poorer removal efficiencies at pH 2 than at pH 3 could be explained with the possible oxonium ion formation at pH 2 due to the strong proton solubility of H_2O_2.

When the removal rates observed in the Fenton and photo-Fenton processes were compared, the positive effect of UV light is evident. In the case of Fenton treatment, at pH 3, the required time to reach about 99% CLZ removal was 60 min (Fig. 2a), whereas it took only 10 min (Fig. 2b). It can safely be stated that UV irradiation (<300 nm) became a mild way to trigger H_2O_2 decomposition which generates $OH^{\bullet}$ compared to Fenton process, as also evidenced by Ghaly et al. [36], Shemer et al. [38] and Rubio et al. [39]. Therefore, more amount of $OH^{\bullet}$ will be generated in the case of photo-Fenton application. Moreover, when exposed to UV light, the Fe^{+3} formed during the Fenton process will lead to the formation of some other species, such as monohydroxy complex $Fe(OH)^{2+}$, which can produce Fe^{2+} and $OH^{\bullet}$ through photosensitization [Eq. (7)] [40].

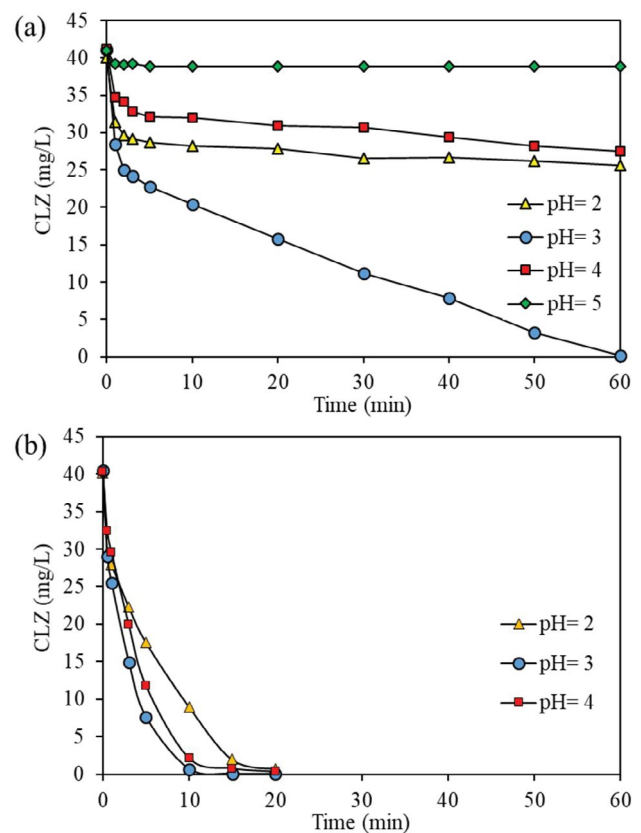$$Fe(OH)^{2+} + h\nu \rightarrow Fe^{2+} + OH^{\bullet} \tag{7}$$

Fig. 2. Time course variation of CLZ concentration at different pH (a) Fenton process (CLZ = 40 mg/L; T = 20°C; H_2O_2 = 100 mg/L; Fe^{2+} = 5 mg/L) and (b) photo-Fenton process (CLZ = 40 mg/L; T = 20°C; H_2O_2 = 50 mg/L; Fe^{2+} = 5 mg/L).

This generated Fe^{2+} could further induce the process, according to Eq. (1). So, these additional sources of $OH^\bullet$ could explain the more rapid depletion of CLZ under the photo-Fenton process as compared to the Fenton process.

3.1.2. Effect of temperature

The effect of temperature on CLZ removal by Fenton oxidation was investigated by working at different temperatures, namely, 10°C, 20°C, 30°C, and 40°C, while keeping the other operational parameters constant. The results obtained are shown in Fig. 3a. As seen from this figure, like for the experimentations performed for the effect of pH, the CLZ concentration declined very rapidly at first (within 1–3 min). Still, then it ceased down gradually (Fig. 3a). This gradual decline ended up at the end of 20 min for the temperature of 40°C, whereas it took 40 and 60 min for 30°C and 20°C cases, respectively. When the temperature was 10°C, the CLZ decline was still going on, though very slowly. So, it was evident that as the temperature increases from 10°C to 40°C, the CLZ removal efficiency increases until 40 min. However, at the end of 60 min, the removal performance belonging to the temperatures of 20°C, 30°C, and 40°C was all the same with almost >99.9%. So, it can be said that the increase in temperature within the studied range has a

positive effect on the removal of CLZ. The efficiency raised from 26% to 99.98% while the temperature rises from 10°C to 40°C at the end of 60 min. It was also seen that degradation occurs in a shorter period when the temperature rises. So, it can be said that the increase in the formation of $OH^\bullet$ with temperature increment, which accelerates the Fenton reaction, will increase the efficiency of the CLZ removal, as also reported by Sun et al. [41]. Fenton applied at room temperature (20°C–25°C) should be preferred even though 40°C of temperature seems to be the most efficient temperature, considering the operating cost.

Photo-Fenton experiments were carried out at different temperatures (20°C, 30°C, and 40°C) while keeping the other operational parameters constant. The results obtained are shown in Fig. 3b. As the temperature rises from 20°C to 30°C and then to 40°C, the removal of CLZ increases at a given time of the experimentation during the first 15 min. This trend was more observable at the 5th min of experimentation. Then after the difference between them diminished, reaching >99% removal at the end of 20 min at all temperatures studied (Fig. 3b). In other words, the initial degradation rate of CLZ gets higher as the temperature increases from 20°C to 40°C.

When compared with the findings of the Fenton process, the stimulatory effect of UV light application is evident in the case of the photo-Fenton process. For example, it took 60 min to achieve >99% CLZ removal at the temperature of 20°C in the Fenton process (Fig. 3a) while it took 20 min at the same temperature in the photo-Fenton process (Fig. 3b). Similarly, at 40°C, >99% CLZ removal was attained at the end of 20 and 10 min in the Fenton and photo-Fenton process, respectively.

3.1.3. Effect of Fe(II)

The experiments were performed using Fe(II) in the range of 2.5–10 mg/L at a fixed H_2O_2 of 100 mg/L, the temperature of 20°C, and pH of 3. The results obtained are shown in Fig. 4. It was evident that as the concentration of Fe^{2+} increases from 2.5 to 10 mg/L, the efficiency of CLZ removal increases in the Fenton oxidation application. With the photo-Fenton application, the CLZ removal efficiency increased as the Fe^{2+} concentration increases as well. But, the positive effect of UV light is evident. In the case of the Fenton process, at Fe^{2+} of 5 mg/L, the required time to reach about 99% CLZ removal was 60 min (Fig. 4a), whereas here it took only 10 min with the photo-Fenton application (Fig. 4b). Moreover, in the case of photo-Fenton, when the concentration of Fe^{2+} is increased from 5 to 7.5 mg/L, no significant change was observed. This could be due to the possibility of the scavenger effect of iron on the generated radicals. Because, when high amounts of Fe^{2+} used, although the formation rate of $OH^\bullet$ by the decomposition of H_2O_2 increases, generated $OH^\bullet$ can also be consumed by the side reactions involving Fe^{3+} [40]. Then, Fe^{3+} will react with the hydroxyl radicals and will form $Fe(OH)_2$, which will, in turn, reduce the effects of the UV source on the degradation of CLZ in photo-Fenton experiments [42]. Moreover, when the iron is used in excess, it will cause a high amount of sludge production besides the high chemical cost. Therefore, the concentration of 5 mg/L Fe^{2+} seems optimal.
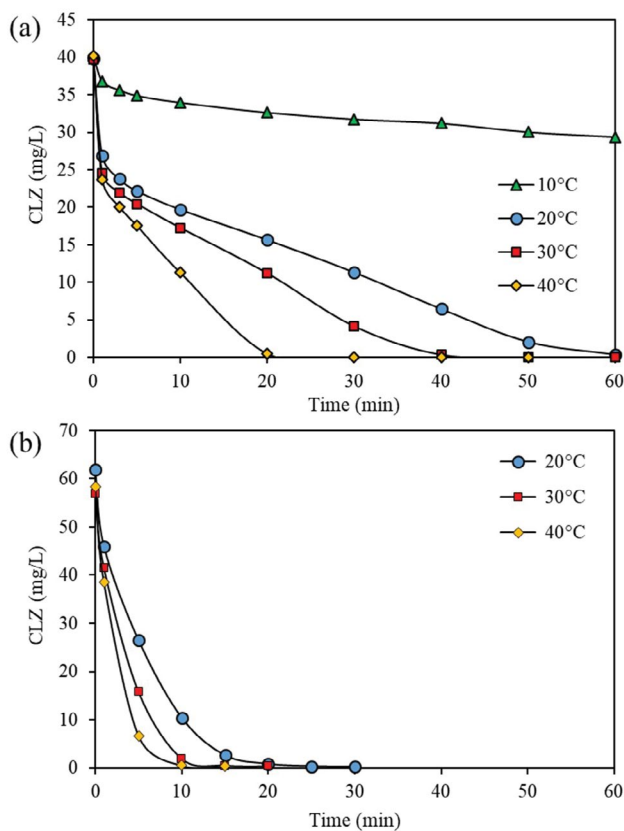
Fig. 3. Time course variation of CLZ concentration at different temperature (a) Fenton process (CLZ = 40 mg/L; H_2O_2 = 50 mg/L; Fe(II) = 5 mg/L; pH = 3) and (b) photo-Fenton process (CLZ = 40 mg/L; H_2O_2 = 50 mg/L; Fe(II) = 5 mg/L; pH = 3).

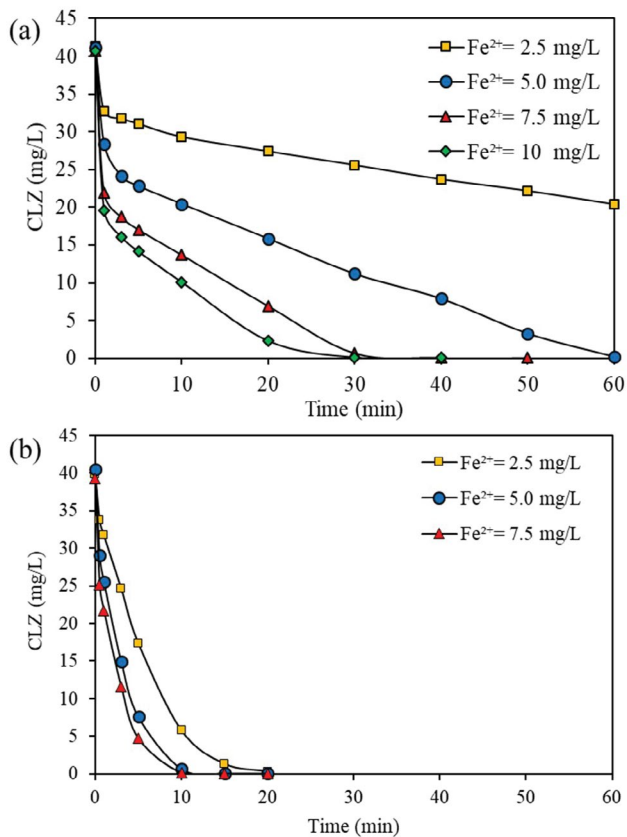Fig. 4. Time course variation of CLZ concentration at different Fe^{2+} (a) Fenton process (CLZ = 40 mg/L; T = 20°C; H_2O_2 = 100 mg/L; pH = 3) (b) photo-Fenton process (CLZ = 40 mg/L; T = 20°C; H_2O_2 = 50 mg/L; pH = 3).
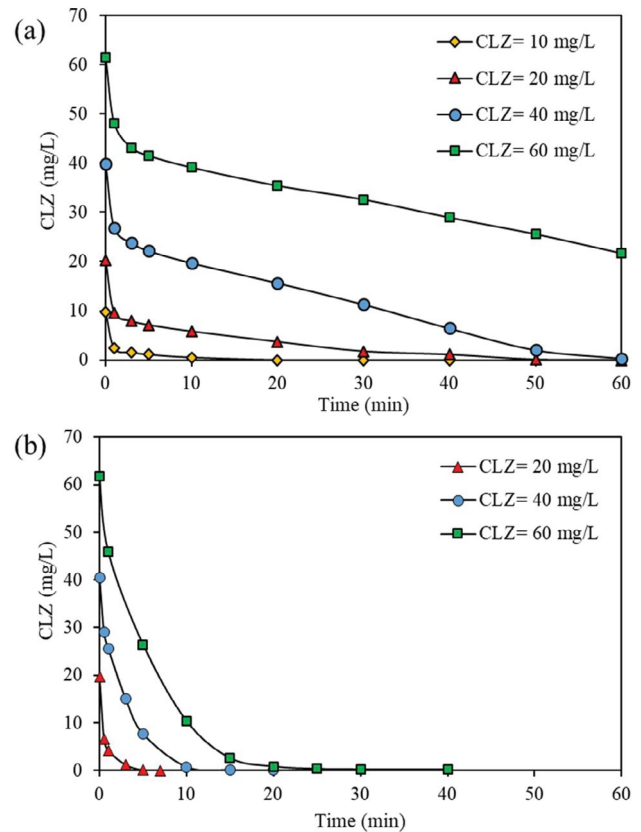
Fig. 5. Time course variation of CLZ for different initial CLZ concentrations by (a) Fenton process (H_2O_2 = 50 mg/L; T = 20°C; Fe^{2+} = 5 mg/L; pH = 3) (b) photo-Fenton process (T = 20°C; H_2O_2 = 50 mg/L; Fe^{2+} = 5 mg/L; pH = 3).

3.1.4. Effect of initial CLZ

The effect of initial CLZ concentration on CLZ removal by the Fenton process was investigated within the concentration range between 10–60 mg/L, as seen in Fig. 5a. The other experimental conditions were maintained as H_2O_2 = 50 mg/L, T = 20°C, Fe^{2+} = 5 mg/L, pH = 3, as to correspond to their optimum values determined previously.

It was evident that as the initial CLZ concentration increases from 10 to 60 mg/L, the CLZ removal efficiency decreases until 40 min. However, at the end of 60 min, the removal performance belonging to the initial CLZ of 10, 20, and 40 mg/L was all the same with almost >99%. The removal efficiency attained for 60 mg/L CLZ was 64% at the end of 60 min, while the removal of CLZ for 10 mg/L CLZ was >99% at the end of 20 min. So, it was clearly seen that when the CLZ concentration increases, the removal efficiency decreases. This was attributed to the fact that there will be no increase in the $OH^{\bullet}$ formed during the reaction when contaminant concentration increases, as also reported by [43].

Fig. 5b shows the effect of initial CLZ concentration (20, 40, and 60 mg/L) on CLZ removal by the photo-Fenton process. The other experimental conditions were maintained as H_2O_2 = 50 mg/L, T = 20°C, Fe^{2+} = 5 mg/L, pH = 3, as to correspond to their optimum values determined. The

CLZ removal efficiency of >99% was achieved at the end of 5 min when the initial CLZ concentration was 20 mg/L, whereas it was 57 and 81% when initial CLZ was 40 and 60 mg/L, respectively. Since the main factor in the removal of CLZ is the amount of $OH^{\bullet}$, which remains stable as the initial Fe^{2+}, and H_2O_2 concentrations are constant during the entire experiments, it is expected to observe the decreasing CLZ removal efficiency while the concentration of CLZ increases. When compared with the Fenton process, at the CLZ concentration of 20 mg/L, >99% removal was possible at the end of 50 min, whereas at the CLZ concentration of 60 mg/L, CLZ removal was only 65% at the end of 60 min. So, the positive effect of UV light is evident.

3.2. Reaction kinetics for Fenton and photo-Fenton experiments

Pseudo-first-order kinetics and BMG reaction kinetics were applied and compared (Figs. 6a and b). The relevant kinetic constants belonging to the optimal conditions determined for Fenton and photo-Fenton processes are provided in Table 3.

As seen from Table 3, compared to pseudo-first-order kinetics, the BMG kinetic model gives the higher correlation coefficients, indicating the better fit of the BMG model to the data. The regression values in the BMG model
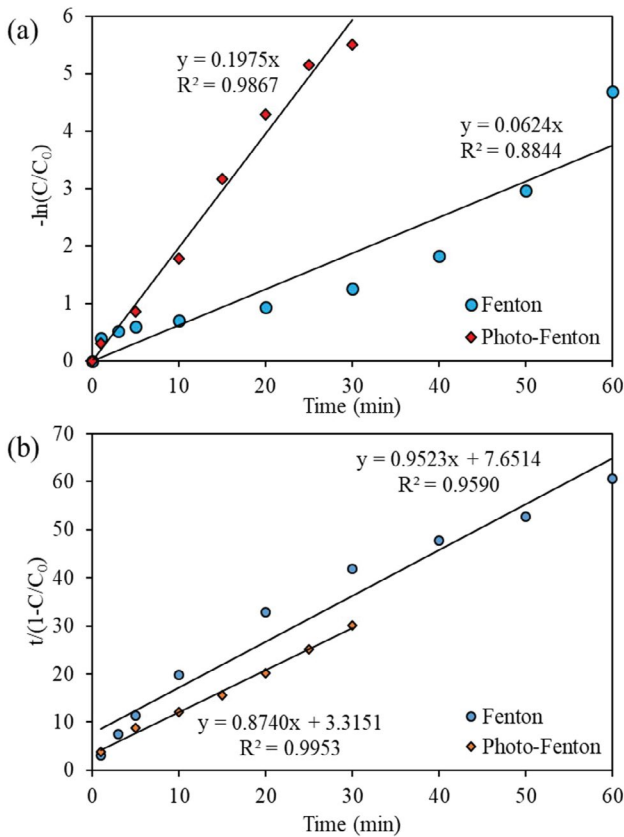
Fig. 6. (a) Pseudo-first-order, and (b) BMG kinetics of CLZ degradation by Fenton and photo-Fenton processes (pH = 3; Fe^{2+} = 5 mg/L; H_2O_2 = 50 mg/L; CLZ = 40 mg/L; T = 20°C for Fenton and pH = 3; Fe^{2+} = 5 mg/L; H_2O_2 = 50 mg/L; CLZ = 60 mg/L; T = 20°C for photo-Fenton).

being higher than 0.95 for both processes prove that the BMG model is followed perfectly. Because of being best fit with BMG kinetic model for the processes, the mathematical equations are derived according to the correlations of operation parameters (Fe^{2+}/ H_2O_2, pH, T, and CLZ concentration) with $1/m$ and $1/b$ values, indicating the initial degradation rate of contaminant and the theoretical maximum contaminant removal, respectively as it was done by Behnajady et al. [27] and Tunç et al. [44]. The equations are presented in Table 4.

3.3. Possible by-products formation of CLZ with Fenton and photo-Fenton processes

In the literature, desphenyl chloridazon (DPC) and methyl desphenyl chloridazon (Me-DPC) are generally observed as by-products of CLZ pesticide degradation [45–47]. According to the European Food Safety Authority (EFSA) [18] report, these by-products are more harmful than its active substance, CLZ. However, when determining the possible by-products, another critical point is to determine the other by-products formed with the further degradation of DPC and Me-DPC. Because these intermediates have

Table 3
Pseudo-first-order and BMG kinetic model parameters for the degradation of CLZ by Fenton and photo-Fenton processes

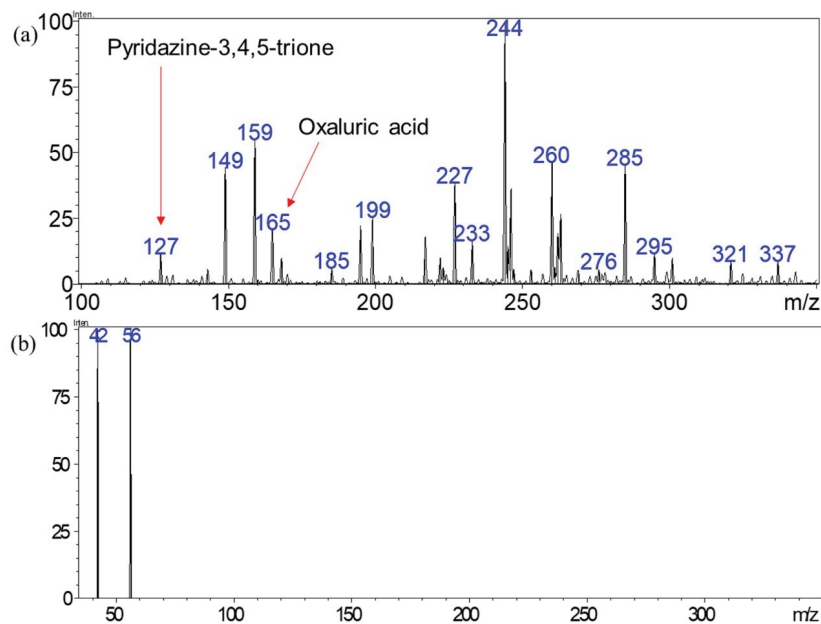| Process	Pseudo-first-order		BMG		
	k_1	R^2	m	b	R^2
Fenton	0.0624	0.8844	7.6514	0.9523	0.959
Photo-Fenton	0.1975	0.9867	3.3151	0.874	0.9953

Fig. 7. (a) LC/MS/MS spectrum of CLZ at the end of Fenton processes (T = 20°C; CLZ = 40 mg/L; H_2O_2 = 50 mg/L; Fe^{2+} = 5 mg/L; pH = 3) and photo-Fenton processes (CLZ = 60 mg/L; H_2O_2 = 50 mg/L; Fe^{2+} = 5 mg/L; pH = 3) and (b) fragment ions of pyridazine-3,4,5-trione (m/z 42 and 56).
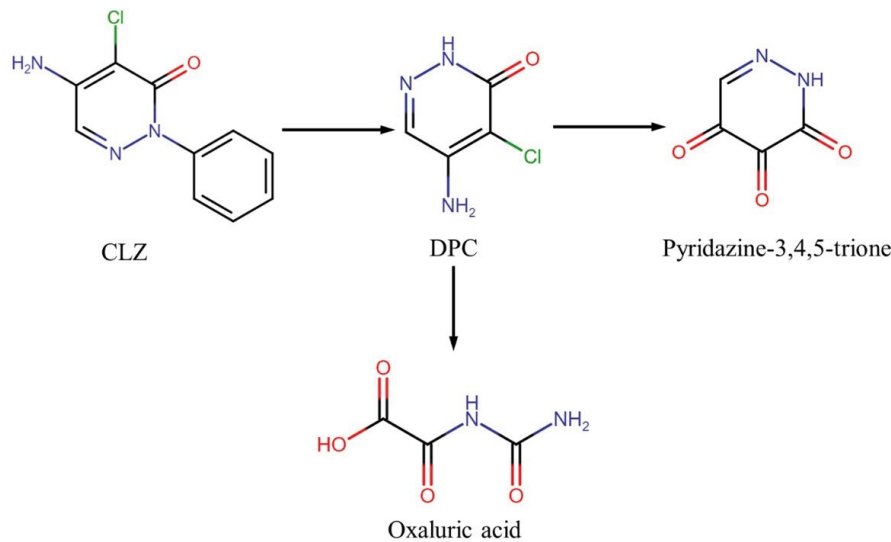
Fig. 8. Possible degradation pathway for the formation of pyridazine-3,4,5-trione and oxaluric acid [5].

the potential to damage the environment. Therefore, in the study, the possible by-products generated by Fenton and photo-Fenton processes were also investigated. During this analysis, it was inspired by a thesis done by Schatz [5] on the CLZ removal by the ozonation process. Schatz [5] identified the possible by-products of CLZ during ozonation and provided the m/z (mass vs. charge) values for the identified products.

For the by-product analysis in the Fenton and photo-Fenton processes, the conditions considered as optimum

were taken into consideration (T = 20°C; CLZ = 40 mg/L; H_2O_2 = 50 mg/L; Fe^{2+} = 5 mg/L; pH = 3 for Fenton and CLZ = 60 mg/L; H_2O_2 = 50 mg/L; Fe^{2+} = 5mg/L; pH = 3 for photo-Fenton). The same evaluation was done in these two processes because there was no difference in the m / z values between the samples taken at 1 h for the Fenton and 30 min for the photo-Fenton processes. Figs. 7a and b show the results obtained from the LC/MS/MS analysis.

It was believed that the compound formed during the Fenton and photo-Fenton processes upon the degradation

Table 4
The correlation equations for $1/m$ and $1/b$ in Fenton and photo-Fenton process

Process	Parameter	Equation	R^2
Fenton	$[Fe^{2+}/H_2O_2]$	$1/m = 35.864[Fe^{2+}/H_2O_2]^2 + 0.233[Fe^{2+}/H_2O_2] + 0.05$	0.99
		$1/b = -211.73[Fe^{2+}/H_2O_2]^2 + 33.202[Fe^{2+}/H_2O_2] - 0.1618$	0.96
		$1/m = -0.0592[Fe^{2+}/H_2O_2]^2 + 0.0097[Fe^{2+}/H_2O_2] + 0.1318$	0.96
		$1/b = 1.8834[Fe^{2+}/H_2O_2]^2 - 1.9162[Fe^{2+}/H_2O_2] + 1.1638$	0.95
	pH	$1/m = -0.0552pH + 0.3024$	0.95
		$1/b = -0.2125pH^2 + 1.3478pH - 1.3899$	0.63
	CLZ	$1/m = 0.0033CLZ^2 - 0.216CLZ + 3.4687$	0.97
		$1/b = -0.001CLZ^2 + 0.0407CLZ + 0.6959$	0.92
	T	$1/m = 0.0272e^{0.0653T}$	0.96
		$1/b = -0.002T^2 + 0.1247T - 0.735$	0.97
Photo-Fenton	$[Fe^{2+}/H_2O_2]$	$1/m = -20.785[Fe^{2+}/H_2O_2]^2 + 10.767[Fe^{2+}/H_2O_2] - 0.248$	1
		$1/b = 26.578[Fe^{2+}/H_2O_2]^2 - 7.305[Fe^{2+}/H_2O_2] + 1.5695$	1
		$1/m = 4.6179[Fe^{2+}/H_2O_2]^2 - 3.7751[Fe^{2+}/H_2O_2] + 0.9522$	1
		$1/b = -1.6004[Fe^{2+}/H_2O_2]^2 + 0.8625[Fe^{2+}/H_2O_2] + 1.0345$	1
	pH	$1/m = -0.2694 pH^2 + 1.642 pH - 1.8806$	1
		$1/b = 0.0557 pH^2 - 0.3278 pH + 1.5864$	1
	CLZ	$1/m = 1.0715e^{-0.023CLZ}$	0.98
		$1/b = -0.0007CLZ^2 + 0.0511CLZ + 0.3755$	1
	T	$1/m = -0.0056T^2 + 0.3408T - 4.1444$	1
		$1/b = -0.0011T^2 + 0.0716T + 0.1053$	1

of DPC is pyridazine-3,4,5-trione, with an m/z value of 127. To prove, the fragments ions were checked. As shown in Fig. 7b, it was proven that the compound is pyridazine-3,4,5-trione, as help from the data provided by Schatz [5]. However, since the ammonium format was used as a buffer during the analysis, which binds 33 numbers to the compound, it was considered that the compound of oxaluric acid with an m/z value of 165 is formed. The presence of DPC is thought to come from the compound with an m/z ratio of 165. Because, in the experimental analysis, it is considered that H_2O is bonded to the compound and bring 19 in number to the DPC with an m/z ratio of 146. In this case, the mechanism of the degradation pathway would be as given in Fig. 8.

4. Conclusions

CLZ removal from waters by Fenton and photo-Fenton processes were studied comparatively. The optimal conditions leading to the highest CLZ removal were identified for both processes. The photo-Fenton process was superior over the Fenton process, considering the removal efficiencies attained. However, one should consider the economic feasibilities of these processes before deciding to choose as a treatment method. In this respect, possible higher sludge production in the Fenton process vs. the additional cost of UV light used in the photo-Fenton process should be evaluated through a pilot-plant study. Removal kinetics followed the BMG kinetics perfectly. By-products, namely, DPC, pyridazine-3,4,5-trione, oxaluric acid, and 5-hydroxyhydantion were identified. For the unidentified by-products, further studies are recommended. Because they might be more toxic than CLZ and may pose a greater danger to the environment. They should be identified and their removal should be investigated further. Thereby, the study will only be complete after these assessments.

References

[1] N. Bensalah, A. Khodary, A. Abdel-Wahab, Kinetic and mechanistic investigations of mesotrione degradation in aqueous medium by Fenton process, J. Hazard. Mater., 189 (2011) 479–485.

[2] G. Buttiglieri, M. Peschka, T. Frömel, J. Müller, F. Malpei, P. Seel, T.P. Knepper, Environmental occurrence and degradation of the herbicide *n*-chloridazon, Water Res., 43 (2009) 2865–2873.

[3] E. González-Pradas, M. Socías-Viciana, M.D. Ureña-Amate, A. Cantos-Molina, M. Villafranca-Sánchez, Adsorption of chloridazon from aqueous solution on heat and acid treated sepiolites, Water Res., 39 (2005) 1849–1857.

[4] A. Khan, N.A. Mir, M. Faisal, M. Muneer, Titanium dioxide-mediated photcatalysed degradation of two herbicide derivatives chloridazon and metribuzin in aqueous suspensions, Int. J. Chem. Eng., 2012 (2012) 8 p, doi: 10.1155/2012/850468.

[5] N.J. Schatz, Ozonation of Chloridazon Metabolites: Identification of Oxidation Products and Reaction Pathways, Doctoral Dissertation, Faculty of Chemistry and Biology, Institute of Karlsruher Technology, Karlsruhe, Germany, 2012.

[6] H. Azaari, R. Chahboune, M. El Azzouzi, M. Sarakha, Elucidation of oxidized products of chloridazon in advanced oxidation processes using a liquid chromatography/negative electrospray ionization tandem mass spectrometric technique, Rapid Commun. Mass Spectrom., 30 (2016) 1145–1152.

[7] S.M. Arnold, W.J. Hickey, R.F. Harris, R.E. Talaat, Integrating chemical and biological remediation of atrazine and s-triazine-containing pesticide wastes, Environ. Toxicol. Chem., 15 (1996) 1255.

[8] J.J. Pignatello, Y.F. Sun, Complete oxidation of metolachlor and methyl parathion in water by the photoassisted Fenton reaction, Water Res., 29 (1995) 1837–1844.

[9] A.C. Silva Costa Teixeira, L. Mendes, G. Stollar, R. Guardani, C.A. Oller Do Nascimento, Photo-Fenton remediation of wastewaters containing agrochemicals, Braz. Arch. Biol. Technol., 48 (2005) 207–218.

[10] E.E. Mitsika, C. Christophoridis, K. Fytianos, Fenton and Fenton-like oxidation of pesticide acetamiprid in water samples: kinetic study of the degradation and optimization using response surface methodology, Chemosphere, 93 (2013) 1818–1825.

[11] F. Gozzi, A. Machulek Jr., V.S. Ferreira, M.E. Osugi, A.P.F. Santos, J.A. Nogueira, R.F. Dantas, S. Esplugas, S.C. de Oliveira, Investigation of chlorimuron-ethyl degradation by Fenton, photo-Fenton and ozonation processes, Chem. Eng. J., 210 (2012) 444–450.

[12] M.S.F. Santos, A. Alves, L.M. Madeira, Paraquat removal from water by oxidation with Fenton's reagent, Chem. Eng. J., 175 (2011) 279–290.

[13] G. Lofrano, L. Rizzo, M. Grassi, V. Belgiorno, Advanced oxidation of catechol: a comparison among photocatalysis, Fenton and photo-Fenton processes, Desalination, 249 (2009) 878–883.

[14] R. Andreozzi, V. Caprio, A. Insola, R. Marotta, Advanced oxidation processes (AOP) for water purification and recovery, Catal. Today, 53 (1999) 51–59.

[15] E. Basturk, M. Karatas, Advanced oxidation of Reactive Blue 181 solution: a comparison between Fenton and Sono-Fenton Process, Ultrason. Sonochem., 21 (2014) 1881–1885.

[16] T. Sruthi, R. Gandhimathi, S.T. Ramesh, P.V. Nidheesh, Stabilized landfill leachate treatment using heterogeneous Fenton and electro-Fenton processes, Chemosphere, 210 (2018) 38–43.

[17] M.I. Badawy, M.Y. Ghaly, T.A. Gad-Allah, Advanced oxidation processes for the removal of organophosphorus pesticides from wastewater, Desalination, 194 (2006) 166–175.

[18] EFSA, Conclusion Regarding the Peer Review of the Pesticide Risk Assessment of the Active Substance Chloridazon, European Food Safety Authority (EFSA), EFSA Scientific Report, 108 (2007) 1–82.

[19] J.R. Bolton, M.I. Stefan, P.-S. Shaw, K.R. Lykke, Determination of the quantum yields of the potassium ferrioxalate and potassium iodide–iodate actinometers and a method for the calibration of radiometer detectors, J. Photochem. Photobiol., A, 222 (2011) 166–169.

[20] N.R. Mohanty, I.W. Wei, Oxidation of 2,4-dinitrotoluene using Fenton's reagent: reaction mechanisms and their practical applications, Hazard. Waste Hazard. Mater., 10 (1993) 171–183.

[21] R. Oliveira, M.F. Almeida, L. Santos, L.M. Madeira, Experimental design of 2,4-dichlorophenol oxidation by Fenton's reaction, Ind. Eng. Chem. Res., 45 (2006) 1266–1276.

[22] F. Yuan, C. Hu, X.X. Hu, J.H. Qu, M. Yang, Degradation of selected pharmaceuticals in aqueous solution with UV and UV/H_2O_2, Water Res., 43 (2009) 1766–1774.

[23] C.M. Sharpless, K.G. Linden, Experimental and model comparisons of low- and medium-pressure Hg lamps for the direct and H_2O_2 assisted UV photodegradation of N-nitrosodimethylamine in simulated drinking water, Environ. Sci. Technol., 37 (2003) 1933–1940.

[24] J.-H. Sun, S.-P. Sun, M.-H. Fan, H.-Q. Guo, L.-P. Qiao, R.-X. Sun, A kinetic study on the degradation of *p*-nitroaniline by Fenton oxidation process, J. Hazard. Mater., 148 (2007) 172–177.

[25] P. Oancea, V. Meltzer, Kinetics of tartrazine photodegradation by UV/H_2O_2 in aqueous solution, Chem. Pap., 68 (2014) 105–111.

[26] C. Lopez-Lopez, J. Martín-Pascual, M.V. Martínez-Toledo, M.M. Muñío, E. Hontoria, J.M. Poyatos, Kinetic modelling of TOC removal by H_2O_2/UV, photo-Fenton and heterogeneous photocatalysis processes to treat dye-containing wastewater, Int. J. Environ. Sci. Technol., 12 (2015) 3255–3262.

[27] M.A. Behnajady, N. Modirshahla, F. Ghanbary, A kinetic model for the decolorization of C.I. Acid Yellow 23 by Fenton process, J. Hazard. Mater., 148 (2007) 98–102.

[28] C.M. Park, J.Y. Heo, Y. Yoon, Oxidative degradation of bisphenol A and 17α-ethinyl estradiol by Fenton-like activity of silver nanoparticles in aqueous solution, Chemosphere, 168 (2017) 617–622.

[29] M. Tamimi, S. Qourzal, N. Barka, A. Assabbane, Y. Ait-Ichou, Methomyl degradation in aqueous solutions by Fenton's reagent and the photo-Fenton system, Sep. Purif. Technol., 61 (2008) 103–108.

[30] E. Neyens, J. Baeyens, A review of classic Fenton's peroxidation as an advanced oxidation technique, J. Hazard. Mater., 98 (2003) 33–50.

[31] A. Babuponnusami, K. Muthukumar, A review on Fenton and improvements to the Fenton process for wastewater treatment, J. Environ. Chem. Eng., 2 (2014) 557–572.

[32] S. Rahim Pouran, A.R. Abdul Aziz, W.M.A. Wan Daud, Review on the main advances in photo-Fenton oxidation system for recalcitrant wastewaters, J. Ind. Eng. Chem., 21 (2015) 53–69.

[33] S. Hashemian, Fenton-like oxidation of malachite green solutions: kinetic and thermodynamic study, J. Chem., 2013 (2013) 7 p, http://dx.doi.org/10.1155/2013/809318.

[34] I. Arslan-Alaton, S. Dogruel, Pre-treatment of penicillin formulation effluent by advanced oxidation processes, J. Hazard. Mater., 112 (2004) 105–113.

[35] P. Saritha, C. Aparna, V. Himabindu, Y. Anjaneyulu, Comparison of various advanced oxidation processes for the degradation of 4-chloro-2 nitrophenol, J. Hazard. Mater., 149 (2007) 609–614.

[36] M.Y. Ghaly, G. Härtel, R. Mayer, R. Haseneder, Photochemical oxidation of p-chlorophenol by UV/H_2O_2 and photo-Fenton process. A comparative study, Waste Manage., 21 (2001) 41–47.

[37] M.S. Lucas, J.A. Peres, Decolorization of the azo dye Reactive Black 5 by Fenton and photo-Fenton oxidation, Dyes Pigm., 71 (2006) 236–244.

[38] H. Shemer, Y.K. Kunukcu, K.G. Linden, Degradation of the pharmaceutical Metronidazole via UV, Fenton and photo-Fenton processes, Chemosphere, 63 (2006) 269–276.

[39] D. Rubio, E. Nebot, J.F. Casanueva, C. Pulgarin, Comparative effect of simulated solar light, UV, UV/H_2O_2 and photo-Fenton treatment ($UV–Vis/H_2O_2/Fe^{2+,3+}$) in the *Escherichia coli* inactivation in artificial seawater, Water Res., 47 (2013) 6367–6379.

[40] X.-R. Xu, X.-Y. Li, X.-Z. Li, H.-B. Li, Degradation of melatonin by UV, UV/H_2O_2, Fe^{2+}/H_2O_2 and $UV/Fe^{2+}/H_2O_2$ processes, Sep. Purif. Technol., 68 (2009) 261–266.

[41] S.-P. Sun, C.-J. Li, J.-H. Sun, S.-H. Shi, M.-H. Fan, Q. Zhou, Decolorization of an azo dye Orange G in aqueous solution by Fenton oxidation process: effect of system parameters and kinetic study, J. Hazard. Mater., 161 (2009) 1052–1057.

[42] A. Bharadwaj, A.K. Saroha, Decolorization of the textile wastewater containing Reactive Blue 19 Dye by Fenton and photo-Fenton oxidation, J. Hazard. Toxic, Radioact. Waste, 19 (2015) 4014043.

[43] N. Modirshahla, M.A. Behnajady, F. Ghanbary, Decolorization and mineralization of C.I. Acid Yellow 23 by Fenton and photo-Fenton processes, Dyes Pigm., 73 (2007) 305–310.

[44] S. Tunç, T. Gürkan, O. Duman, On-line spectrophotometric method for the determination of optimum operation parameters on the decolorization of Acid Red 66 and Direct Blue 71 from aqueous solution by Fenton process, Chem. Eng. J., 181–182 (2012) 431–442.

[45] S. Kowal, P. Balsaa, F. Werres, T.C. Schmidt, Fully automated standard addition method for the quantification of 29 polar pesticide metabolites in different water bodies using LC-MS/MS, Anal. Bioanal. Chem., 405 (2013) 6337–6351.

[46] A. Schuhmann, O. Gans, S. Weiss, J. Fank, G. Klammler, G. Haberhauer, M.H. Gerzabek, A long-term lysimeter experiment to investigate the environmental dispersion of the herbicide chloridazon and its metabolites—comparison of lysimeter types, J. Soils Sediments, 16 (2016) 1032–1045.

[47] A. Mbiri, G. Wittstock, D.H. Taffa, E. Gatebe, J. Baya, M. Wark, Photocatalytic degradation of the herbicide chloridazon on mesoporous titania/zirconia nanopowders, Environ. Sci. Pollut. Res., 25 (2018) 34873–34883.